UC Irvine

Title

Modal Propagation and Excitation on a Wire-Medium Slab

Authors

Burghignoli, Paolo
Lovat, Giampiero
Capolino, Filippo
et al.

Peer reviewed

Modal Propagation and Excitation on a Wire-Medium Slab

Paolo Burghignoli, *Senior Member, IEEE*, Giampiero Lovat, *Member, IEEE*,
Filippo Capolino, *Senior Member, IEEE*, David R. Jackson, *Fellow, IEEE*, and Donald R. Wilton, *Life Fellow, IEEE*

Abstract—A grounded wire-medium slab has recently been shown to support leaky modes with azimuthally independent propagation wavenumbers capable of radiating directive omni-directional beams. In this paper, the analysis is generalized to wire-medium slabs in air, extending the omnidirectionality properties to even modes, performing a parametric analysis of leaky modes by varying the geometrical parameters of the wire-medium lattice, and showing that, in the long-wavelength regime, surface modes cannot be excited at the interface between the air and wire medium. The electric field excited at the air/wire-medium interface by a horizontal electric dipole parallel to the wires is also studied by deriving the relevant Green's function for the homogenized slab model. When the near field is dominated by a leaky mode, it is found to be azimuthally independent and almost perfectly linearly polarized. This result, which has not been previously observed in any other leaky-wave structure for a single leaky mode, is validated through full-wave moment-method simulations of an actual wire-medium slab with a finite size.

Index Terms—Leaky modes, metamaterials, near field, planar slab, wire medium.
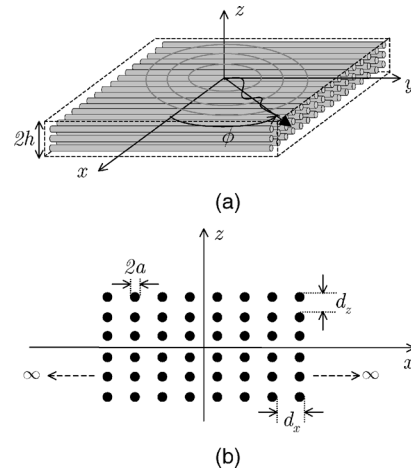
Fig. 1. (a) Wire-medium slab in air with the relevant coordinate axes. (b) Transverse view of the wire-medium slab with the relevant geometrical parameters.

I. INTRODUCTION

THE 1-D *wire medium* consists of a periodic arrangement of thin perfectly conducting cylinders (wires), infinitely long and parallel, embedded inside a homogeneous host dielectric medium. Such an artificial medium, also known as a *rodded medium*, has been known since the 1950s to be described in the long-wavelength regime by a scalar permittivity with a plasma-like dispersion behavior for waves having the electric field polarized along the axis of the wires [1].

As can easily be predicted from the directionality of the wire lattice, the 1-D wire medium is uniaxial for waves with arbitrary polarization. A far less trivial property, first pointed out in [2] and [3], is the presence of spatial dispersion even in the large wavelength regime, i.e., the nonlocal nature of the electrical response of the wire medium. This feature, also present in more complex 2-D and 3-D wire arrangements [4], [5], has remarkable consequences on the propagation of plane waves inside an unbounded 1-D wire medium: for instance, in addition

to the usual ordinary and extraordinary waves existing in any uniaxial medium (TE and TM with respect to the wire direction, respectively), an additional TEM wave may exist, propagating in the direction of the wires; furthermore, for extraordinary plane waves, the propagation wavenumber does not depend on the direction of propagation of the wave, i.e., the isofrequency surfaces in the wavenumber space are spherical [3]. The presence of spatial dispersion poses a formidable challenge in the solution of boundary-value problems with nonplanar boundaries. Even in the presence of purely planar interfaces, additional boundary conditions may be required when the wires are not purely parallel to the interfaces [6]. Propagation of waves in bounded wire-medium structures has been considered in [7] and [8].

In this paper, we consider the problem of modal excitation and propagation along a canonical planar waveguide, a slab in free space, made of a 1-D wire medium with wires parallel to the air–slab interfaces (see Fig. 1, where the relevant geometrical parameters and the adopted coordinate system are also shown). Recently, certain properties of a grounded configuration of such a slab have been studied, excited by a simple electric dipole source placed inside the wire-medium and oriented parallel to the wires [9]. For frequencies slightly above the plasma frequency, where the relative permittivity is positive but small, it has been shown that the structure is capable of producing narrow-beam radiation patterns. Depending on the frequency, the beam may be either a pencil beam at broadside, or a conical beam at a particular scan angle. It was shown in [10] and [11] that this directive radiation is due to the excitation of a leaky

mode supported by the grounded slab having a wavenumber independent of its azimuthal angle of propagation.

The aim of this paper is twofold. First, to generalize the analysis of modal propagation at arbitrary angles to the case of a wire-medium slab in air, considering both even and odd modes, performing a *parametric analysis* of the properties of the leaky modes, and showing that *surface* (either ordinary or plasmonlike) modes cannot propagate along the slab in the long-wavelength regime. Second, to consider the *excitation* of a dominant leaky mode by a horizontal dipole source parallel to the wires, and to study the properties of the resulting *near field* at the air–slab interface, adopting both a homogeneous model and a full-wave method of moments (MoM) approach.

This paper is organized as follows. In Section II, the homogenized model of the wire-medium slab is presented along with the relevant transverse equivalent networks; these allow for a discussion of the properties of surface and leaky modes and of the electric field excited at the air–slab interface by a horizontal electric dipole. In Section III, the adopted full-wave modal analysis based on the MoM in the spatial domain is described. In Section IV, numerical results for the propagation of leaky modes and for the features of the electric field excited by the dipole source are presented. Finally, in Section V, conclusions are drawn.

II. HOMOGENIZED MODEL AND TRANSVERSE EQUIVALENT NETWORK

A. Homogenized Medium

The wire medium shown in Fig. 1 is anisotropic for electromagnetic waves with an arbitrary polarization, requiring the use of a uniaxial permittivity dyadic with optical axis directed parallel to the wire (y) axis when it is homogenized at wavelengths sufficiently larger than the wire spacing. Actually, as shown in [2] and [3], not only anisotropy, but also spatial dispersion needs to be included in a homogenized description of the medium, even for large wavelengths. The effective permittivity dyadic thus depends on both the frequency and wavenumber, and for thin wires [i.e., $a \ll \min(d_x, d_z)$] and in the large-wavelength limit (i.e., $\max(d_x, d_z) \ll \lambda_0$, with λ_0 the free-space wavelength), it reads

$$
\begin{aligned}
\underline{\underline{\varepsilon}} &= \varepsilon_0 \left[\varepsilon_{ryy} \mathbf{u}_y \mathbf{u}_y + \varepsilon_{rt} (\mathbf{u}_x \mathbf{u}_x + \mathbf{u}_z \mathbf{u}_z) \right] \\
&= \varepsilon_0 \varepsilon_{rh} \left[\left(1 - \frac{k_p^2}{\varepsilon_{rh} k_0^2 - k_y^2} \right) \mathbf{u}_y \mathbf{u}_y + \mathbf{u}_x \mathbf{u}_x + \mathbf{u}_z \mathbf{u}_z \right]
\end{aligned} \quad (1)
$$

where ε_{rh} is the relative permittivity of the medium hosting the wires (for the structures considered here, air is assumed as the host medium, i.e., $\varepsilon_{rh} = \varepsilon_{rt} = 1$), k_0 is the free-space wavenumber, k_p is the plasma wavenumber, and k_y is the wavenumber along the wire axis. Here and in the following, boldface symbols denote vectors, while $\mathbf{u}_x$, $\mathbf{u}_y$, and $\mathbf{u}_z$ denote unit vectors along the x-, y-, and z-directions, respectively. The plasma wavenumber is given by (see [12])

$$
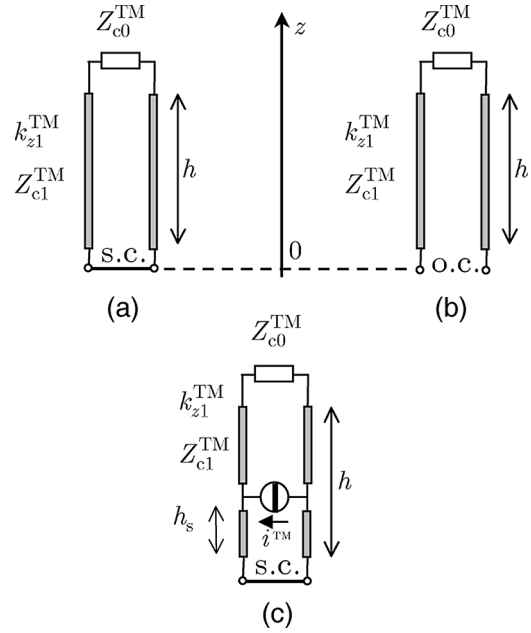k_p = \frac{\sqrt{2\pi}}{s} \frac{1}{\sqrt{\ln \frac{s}{2\pi a} + F(\nu)}} \quad (2)
$$

Fig. 2. Transverse equivalent network representations of a wire-medium slab in air with thickness $2h$ for: (a) odd TM_y modes and (b) even TM_y modes. (c) Transverse equivalent network for a grounded wire-medium slab as in (a) with thickness h, excited by a horizontal electric dipole parallel to the wires placed at a distance h_s from the ground plane.

where $s = \sqrt{d_x d_z}$, $\nu = d_x / d_z$, and

$$
F(\nu) = -\frac{1}{2} \ln(\nu) + \sum_{n=1}^{+\infty} \frac{1}{n} \left[\coth(\pi n \nu) - 1 \right] + \frac{\pi \nu}{6}. \quad (3)
$$

In particular, for square lattices, i.e., when $d_x = d_z$ ($\nu = 1$), there results $F(1) \simeq 0.527$, while when $d_x = 2d_z$ or $d_x = d_z/2$, there results $F(2) = F(0.5) \simeq 0.7$.

B. Modal Dispersion Equations and Surface-Wave Suppression

The field of a leaky mode propagating on a wire-medium slab, as in Fig. 1, with complex wavenumber $k_\rho^{\mathrm{LW}} = \beta - j\alpha$ at an angle ϕ has an exponential dependence on the x- and y-coordinates with wavenumbers $k_x = k_\rho^{\mathrm{LW}} \cos \phi$ and $k_y = k_\rho^{\mathrm{LW}} \sin \phi$. The electromagnetic field inside the air region and the wire-medium slab is decomposed into TE_y and TM_y components, which can be represented through equivalent transmission lines along z (details are given in the Appendix).

The TE_y (ordinary) polarization sees an isotropic equivalent medium equal to the host medium (air). Furthermore, as shown in [10] and [11], at the air/wire-medium interface, no $\mathrm{TE}_y/\mathrm{TM}_y$ coupling occurs when the host medium is air. Therefore, TE_y and TM_y polarizations are decoupled and TE_y *modal* solutions are not supported by the wire-medium slab. (For completeness, we note here that *nonmodal* TE_y solutions exist, which are actually TEM_ρ plane waves propagating in free space at arbitrary angles ϕ in the xy-plane with no z variation).

The study of TM_y modes in a slab of thickness $2h$ is performed using the transverse equivalent networks shown in Fig. 2(a) and (b) for odd and even modes; by symmetry, the plane $z = 0$ is equivalent to a perfect electric conductor for odd

modes and to a perfect magnetic conductor for even modes. The transverse equivalent network parameters are

$$k_{z0}^{\mathrm{TM}} = \sqrt{k_0^2 - k_\rho^2}$$
$$k_{z1}^{\mathrm{TM}} = \sqrt{k_0^2 - k_{\mathrm{p}}^2 - k_\rho^2} \qquad (4)$$

and

$$Z_{\mathrm{c0}}^{\mathrm{TM}} = \frac{\eta_0}{k_0} \frac{k_0^2 - k_\rho^2 \sin^2\phi}{k_{z0}^{\mathrm{TM}}}$$
$$Z_{\mathrm{c1}}^{\mathrm{TM}} = \frac{\eta_0}{k_0} \frac{k_0^2 - k_\rho^2 \sin^2\phi}{k_{z1}^{\mathrm{TM}}} \qquad (5)$$

where η_0 is the free-space characteristic impedance. As concerns the value of the parameter h, i.e., the equivalent thickness of the homogenized slab, we have adopted here the choice $2h = Nd_z$, where N is the number of wire layers along the z-direction; although quite natural [13], this choice has no rigorous justification, but it will be seen in Section IV to yield results in good agreement with the full-wave simulations.

The modal dispersion equations for the extraordinary even and odd TM_y modes can be obtained by enforcing the condition of resonance on the transverse equivalent networks shown in Fig. 2(a) and (b), i.e.,

$$\frac{1}{Z_{\mathrm{c0}}^{\mathrm{TM}}} + j\frac{1}{Z_{\mathrm{c1}}^{\mathrm{TM}}} \tan\left(k_{z1}^{\mathrm{TM}}h\right) = 0 \text{ (even modes)}$$
$$Z_{\mathrm{c0}}^{\mathrm{TM}} + jZ_{\mathrm{c1}}^{\mathrm{TM}} \tan\left(k_{z1}^{\mathrm{TM}}h\right) = 0 \text{ (odd modes).} \qquad (6)$$

From (6) and (5), it can be seen that a possible solution is $k_\rho = k_0/\sin\phi$, which corresponds to having $k_y = k_0$. The case $k_y = k_0$ corresponds to TEM_y waves, and represents a special case for which the permittivity model in (1) breaks down for a practical medium since this equation predicts that $\varepsilon_{\mathrm{r}yy} = \infty$ for such waves (for an idealized medium that obeys (1), a continuous nonmodal spectrum of TEM_y waves may be shown to exist [3]). For $k_y \neq k_0$, from (4) and (5), the dispersion equations (6) can be written as

$$k_{z1}^{\mathrm{TM}} - jk_{z0}^{\mathrm{TM}} \cot\left(k_{z1}^{\mathrm{TM}}h\right) = 0 \text{ (even modes)}$$
$$k_{z1}^{\mathrm{TM}} + jk_{z0}^{\mathrm{TM}} \tan\left(k_{z1}^{\mathrm{TM}}h\right) = 0 \text{ (odd modes)} \qquad (7)$$

which turn out to be independent of the propagation angle ϕ (and equal to the dispersion equation for TE_z modes of an ordinary isotropic slab with $\varepsilon_{\mathrm{r}} = 1 - k_{\mathrm{p}}^2/k_0^2$). This interesting property arises from the fact that the ϕ dependence in both of the characteristic impedance terms of (5) are the same, and hence, this dependence cancels out when these terms are inserted into the transverse resonance equation.

From the omnidirectionality of modal propagation, important conclusions can be drawn about the existence of bound waves (*surface waves*) on the wire-medium slab with air as the host medium. Let us consider first propagation in the direction orthogonal to the wire aixs. By symmetry, the electromagnetic field of TM_y modes propagating in this direction has nonzero components E_y, H_x, and H_z (so that these modes can also be classified as TE_z); from (1), it is then found that such modes see the homogenized medium as an isotropic medium with a

plasma-like scalar relative permittivity $\varepsilon_{\mathrm{r}} = 1 - k_{\mathrm{p}}^2/k_0^2$. Now, when $k_0 < k_{\mathrm{p}}$ (i.e., the frequency is lower than the plasma frequency), it follows that $\varepsilon_{\mathrm{r}} < 0$, i.e., the medium is epsilon negative; therefore, TE_z (i.e., TM_y) surface waves cannot propagate (a proof may be found in [14] for odd modes with the extension to even modes being straightforward). On the other hand, when $k_0 > k_{\mathrm{p}}$ (i.e., the frequency is higher than the plasma frequency), the medium has a relative permittivity that is positive, but lower than one, so that total reflection cannot occur at the slab–air interface, and again, no surface waves may exist.

Therefore, as long as the homogenization process is valid, surface waves cannot propagate orthogonally to the wires. By virtue of the omnidirectionality of modal propagation established above, it can be concluded that surface waves cannot propagate at any frequency and at any angle along a wire-medium slab in air. The only type of guided mode that may, therefore, exist on the homogenized wire medium slab is a TM_y leaky wave. The properties of such a mode are explored in Section IV-A.

C. Electric Field at the Air–Slab Interface

Assuming now the presence of a horizontal infinitesimal electric dipole parallel to the wires, we wish to calculate the electric field at the air–slab interface, still assuming a homogenized model for the slab. Although a rigorous calculation of such a near field would require a full-wave treatment of the interaction between the aperiodic dipole source and its periodic wire-medium environment, e.g., through the array scanning method [15], the results obtained with the homogenized model may help in gaining physical insight into the radiation mechanism of the structure. Furthermore, as will be shown in Section IV-B, when the near field is dominated by a leaky mode, the homogenized results are in good agreement with those obtained via a rigorous full-wave analysis.

The field excited by a dipole parallel to the metal wires is purely TM_y (since by reciprocity neither TE_y nor TEM_y fields can be excited), and its tangential components $\widetilde{E}_x$ and $\widetilde{E}_y$ at $z = h$ can be calculated from the spectral form of Maxwell's equations (21) and (22) and from (27) as

$$\widetilde{E}_y(k_x, k_y) = V_i^{\mathrm{TM}}(k_x, k_y) \left[-\widetilde{J}_y(k_x, k_y))\right] = -V_i^{\mathrm{TM}}(k_x, k_y)$$
$$\widetilde{E}_x(k_x, k_y) = -\frac{k_x k_y}{k_0^2 - k_y^2}\widetilde{E}_y(k_x, k_y) = \frac{k_x k_y}{k_0^2 - k_y^2}V_i^{\mathrm{TM}}(k_x, k_y) \qquad (8)$$

where $\widetilde{J}_y = 1$ [A] for an elemental electric dipole directed along y. The TM_y equivalent voltage V_i^{TM} at $z = h$ due to a 1-A equivalent impressed current at $z = h_{\mathrm{s}}$ [see Fig. 2(c)] is given by

$$V_i^{\mathrm{TM}}(k_x, k_y) = \frac{j\eta_0}{k_0} \frac{(k_0^2 - k_y^2)\sin(k_{z1}^{\mathrm{TM}}h_{\mathrm{s}})}{k_{z1}^{\mathrm{TM}}\cos(k_{z1}^{\mathrm{TM}}h) + jk_{z0}^{\mathrm{TM}}\sin(k_{z1}^{\mathrm{TM}}h)}. \qquad (9)$$

It is interesting to note that

$$V_i^{\mathrm{TM}}(k_x, k_y) = \left(1 - \frac{k_y^2}{k_0^2}\right)V_i^{\mathrm{TE}_z}(k_\rho) \qquad (10)$$

where $V_i^{\text{TE}_z}$ is the TE_z equivalent voltage due to a 1-A current source for an *isotropic* slab with relative permittivity $\varepsilon_{\text{r}} = 1 - k_{\text{p}}^2/k_0^2$. Since, as is well known, $V_i^{\text{TE}_z}$ depends only on the radial wavenumber k_ρ, the anisotropy of the structure appears only in the factor $(k_0^2 - k_y^2)$ in the numerator of (9).

The tangential components of the electric field at $z = h$ can be calculated in the spatial domain by inverse Fourier transforming (8), i.e.,

$$E_y(x, y) = \iint_{\mathbb{R}} -\frac{V_i^{\text{TM}}(k_x, k_y)}{(2\pi)^2} e^{-j(k_x x + k_y y)} \, dk_x \, dk_y$$

$$E_x(x, y) = \iint_{\mathbb{R}} \frac{k_x k_y}{k_0^2 - k_y^2} \frac{V_i^{\text{TM}}(k_x, k_y)}{(2\pi)^2} e^{-j(k_x x + k_y y)} dk_x \, dk_y. \tag{11}$$

By performing the standard change of variables in the transverse plane from rectangular to polar in both the spectral and spatial domains [17], from (11) and (10) we obtain for the electric field excited at the air–slab interface by the considered elemental source

$$E_y(x, y) = -\frac{1}{8\pi} \int_{-\infty}^{+\infty} V_i^{\text{TE}_z}(k_\rho) \left(2k_\rho - \frac{k_\rho^3}{k_0^2} \right) H_0^{(2)}(k_\rho \rho) \, dk_\rho$$

$$-\frac{1}{8\pi} \cos(2\phi) \int_{-\infty}^{+\infty} V_i^{\text{TE}_z}(k_\rho) \frac{k_\rho^3}{k_0^2} H_2^{(2)}(k_\rho \rho) \, dk_\rho \tag{12}$$

and

$$E_x(x, y) = -\frac{1}{8\pi} \sin(2\phi) \int_{-\infty}^{+\infty} V_i^{\text{TE}_z}(k_\rho) \frac{k_\rho^3}{k_0^2} H_2^{(2)}(k_\rho \rho) \, dk_\rho. \tag{13}$$

The integrands in (12) and (13) have pole singularities in the complex k_ρ plane corresponding to the leaky modes supported by the structure, and branch-point singularities of square-root type at $k_\rho = \pm k_0$, which give rise to the space-wave contribution [17]. Moreover, there is a branch point at the origin due to the presence of the Hankel functions; however, with a suitable choice of the relevant branch cut (along the imaginary axis), this branch cut lies along the usual Sommerfeld branch cut for the k_0 wavenumber [17], and hence, is of no concern in what follows.

As is well known, by deforming the original integration path along the real axis to a vertical pair of paths through the branch point at k_0, the components of the total field in (12) and (13) can be decomposed as the sum of a surface-wave field, a leaky-wave field, and a space-wave field [17]

$$\mathbf{E} = \mathbf{E}^{\text{SW}} + \mathbf{E}^{\text{LW}} + \mathbf{E}^{\text{SpW}}. \tag{14}$$

The leaky-wave field is given by the sum of the residue contributions at the complex poles, which are captured by the above-mentioned integration-path deformation; moreover, in the present case, the surface-wave field is absent so that

$$\mathbf{E} = \sum_n \mathbf{E}_n^{\text{LW}} u_n + \mathbf{E}^{\text{SpW}} \tag{15}$$

where u_n is equal to 1 if the nth leaky-wave pole is captured, otherwise it is zero. When only one term in the sum is significant, the corresponding leaky mode is said to be dominant. Finally, the space-wave field is given by the integral along the above-mentioned vertical paths through the branch point at k_0.

The contribution of the dominant leaky mode to the total field excited by the considered source is evaluated as the residue contribution to the integrals in (12) and (13) at the dominant complex leaky-wave pole $k_\rho^{\text{LW}} = \beta - j\alpha$ (i.e., the one with the lowest attenuation constant α) and it has the expression

$$E_y^{\text{LW}}(x, y) = -\frac{1}{4} E_0 \left(2k_\rho^{\text{LW}} - \frac{(k_\rho^{\text{LW}})^3}{k_0^2} \right) H_0^{(2)}(k_\rho^{\text{LW}} \rho)$$

$$-\frac{1}{4} \cos(2\phi) E_0 \frac{(k_\rho^{\text{LW}})^3}{k_0^2} H_2^{(2)}(k_\rho^{\text{LW}} \rho) \tag{16}$$

and

$$E_x^{\text{LW}}(x, y) = -\frac{1}{4} \sin(2\phi) E_0 \frac{(k_\rho^{\text{LW}})^3}{k_0^2} H_2^{(2)}(k_\rho^{\text{LW}} \rho) \tag{17}$$

where $E_0 = -j \text{Res} \left[V_i^{\text{TE}_z}(k_\rho) \right]_{k_\rho = k_\rho^{\text{LW}}}$.

Numerically, the integrations in (12) and (13) are performed by suitably deforming the integration path to avoid the branch-point singularity located at $k_\rho = k_0$ on the real axis and by adopting standard adaptive quadrature routines. The residue term in (16) and (17) can instead be evaluated by numerical integration of the function $V_i^{\text{TE}_z}(k_\rho)$ along a small circle enclosing the relevant leaky-wave pole $k_\rho = k_\rho^{\text{LW}}$. Finally, the space-wave field is calculated through the numerical integration of the integrand of (12) and (13) along a vertical pair of paths through the branch point at $k_\rho = k_0$; for large distances from the source, this path becomes a steepest descent path along which the integrand decays exponentially fast [17].

It is noted that in the second addend in (16), as well as the cross-polarized term in (17), the terms in front of the Hankel functions are proportional to $k_\rho^{\text{LW}3}$ for small values of k_ρ^{LW}. Note that when the leaky mode has a small propagation wavenumber so that $|k_\rho^{\text{LW}}| \ll k_0$, the weighting coefficients from the k_ρ terms are such that the cross-polarized field of the leaky mode is negligible. The wavenumber will be small when the permittivity $\varepsilon_{\text{r}yy}$ is small (corresponding to a weakly attenuated leaky mode that radiates near broadside).

The space-wave field excited by the source is mainly associated with the branch point at $k_\rho = k_0$, and hence, k_ρ is not small for this wave. Therefore, the space-wave field has significant cross-polarization. In fact, this field will mainly be polarized perpendicular to the wires since the wires will act to short out the parallel component of the field for this wave. However, if the leaky mode is dominant, the overall field will exhibit a good polarization purity. This will be the case when the permittivity $\varepsilon_{\text{r}yy}$ is small, as will be demonstrated later in the results. These points explain why the radiation patterns in [9]–[11] have a good polarization purity.

III. Full-Wave Modal Analysis

Leaky-wave propagation on the wire-medium slab with air as the host medium is also studied here by means of a rigorous

formulation based on the MoM in the spatial domain. The periodicity of the structure allows for considering one spatial period only (unit cell), thus requiring the use of a periodic (free-space) Green's function G_p. Since the latter is known to be represented by a slowly convergent series, an effective numerical acceleration procedure has been implemented based on the Ewald summation technique [16].

As mentioned in Section II, when the host medium is air, TE_y and TM_y polarizations do not couple, and they can be studied separately. Furthermore, for *very thin* wires (as the ones considered here), only the TM_y polarization is of interest since, in this limit, the TE_y polarization does not interact with the wires and propagates as in free space (and therefore no TE_y modes exist). It should also be noted that for the discrete wire-medium structure shown in Fig. 1, TEM_y multiconductor transmission line modes may exist, which are different than the modal TM_y radially propagating solutions that are examined here. However, such modes will not be considered in the following since they cannot be excited by an electric dipole that is parallel to the wires (the type of source considered here). This follows from reciprocity since the dipole is orthogonal to the electric field of these modes.

Due to the exponential dependence of the modal field on the x- and y-coordinates and the invariance of the structure along the y-direction, the electromagnetic problem is reduced to a 2-D one in the xz-plane. Moreover, for the TM_y polarization of interest, the azimuthal component J_ℓ of the current along the wires is identically zero and the MoM unknown is thus the longitudinal component J_y. The electric field integral equation (EFIE) for wave propagation at an arbitrary angle ϕ reads (see [11, Appendix])

$$\sqrt{k_0^2 - k_y^2} \int_\mathcal{C} J_y(\boldsymbol{r}') G_\mathrm{p}\!\left(\sqrt{k_0^2 - k_y^2}\, |\boldsymbol{r} - \boldsymbol{r}'|\right) \mathrm{d}\ell' = 0, \qquad \boldsymbol{r} \in \mathcal{C} \tag{18}$$

where $\mathcal{C}$ indicates the union of the boundaries of the wire cross sections in a unit cell, while $\boldsymbol{r} = x\mathbf{u}_x + z\mathbf{u}_z$ and $\boldsymbol{r}' = x'\mathbf{u}_x + z'\mathbf{u}_z$ are the observation and source vectors in the xz-plane, respectively. Since $k_y = k_\rho^\mathrm{LW} \sin\phi$, from (18) it is immediately seen that the EFIE for wave propagation at an arbitrary angle ϕ is equivalent to that at an angle of $\phi = 0°$ (propagation orthogonal to the wires, i.e., no variation of currents or fields with y) provided that the free-space wavenumber k_0 is replaced by a scaled effective wavenumber $k_\mathrm{eff} = \sqrt{k_0^2 - k_y^2}$. Finally, the propagation along x determines the phasing $k_x = k_\rho^\mathrm{LW} \cos\phi$ used in the periodic Green's function G_p.

The EFIE can be discretized using subdomain (e.g., piecewise constant) basis functions and a Galerkin testing procedure. However, because of the simple (circular) cross section of the wires, entire-domain basis functions can also be effectively used, dramatically reducing the computational effort and the size of the MoM matrix. In particular, exponential functions have been used to expand the unknown current density J_y so that for each cylinder

$$J_y(\boldsymbol{r}) = J_y(r, \gamma) = \frac{\delta(r-a)}{r}\, \hat{J}_y(\gamma)$$

$$\hat{J}_y(\gamma) = \sum_{m=-\infty}^{+\infty} i_m e^{jm\gamma} \tag{19}$$

where (r, γ) are polar coordinates in the xz-plane centered on the wire axis, a is the wire radius, and i_m are the unknown expansion coefficients. Since the wires are very thin, typically very few basis functions are needed to obtain an accurate representation of the current density; in the simulations, three basis functions (i.e., $m = 0, \pm 1$) have been used, although using only the $m = 0$ basis function would yield sufficiently accurate results. Once the EFIE has been discretized, the complex wavenumber $k_\rho^\mathrm{LW} = \beta - j\alpha$ of the leaky modes supported by the wire-medium slab has then been determined by searching for the zeros of the determinant (as a function of k_ρ) of the coefficient matrix of the resulting linear system.

As long as the period is much smaller than the wavelength and (1), the leaky mode has a fundamental Floquet wave that is *improper* (exponentially increasing in the vertical z-direction), while all other Floquet waves are proper (exponentially decreasing in the z direction); this means that, in the calculation of the spectral part of the periodic Green's function in the Ewald representation, the determination of the square root defining the pth transverse harmonic

$$k_{z,\mathrm{p}} = \sqrt{k_\mathrm{eff}^2 - k_{x,\mathrm{p}}^2}$$
$$= \sqrt{k_0^2 - (k_\rho^\mathrm{LW})^2 \sin^2\phi - \left(k_\rho^\mathrm{LW} \cos\phi + \frac{2\pi\mathrm{p}}{d_x}\right)^2} \tag{20}$$

has to be correctly chosen. In particular, $\Im\mathrm{m}\{k_{z,0}\} > 0$ for the fundamental zeroth harmonic and $\Im\mathrm{m}\{k_{z,\mathrm{p}}\} < 0$ for all the other harmonics (i.e., $p = \pm 1, \pm 2, \ldots$) [18].

IV. NUMERICAL RESULTS

A. Parametric Analysis of Leaky Modes

To validate the conclusions reached with the homogenized model of the wire-medium slab, a parametric investigation of modal propagation has been performed through the rigorous moment-method approach described in Section III.

In Fig. 3, dispersion curves for the fundamental even (TM_1) and odd (TM_2) modes are reported for propagation orthogonal ($\phi = 0°$) and parallel ($\phi = 90°$) to the wires (*black lines*), along with the corresponding curves obtained by means of the homogenized model (*gray lines*). (The notation even/odd refers to the variation of the transverse electric field about the center of the slab. At cutoff, the TM_1 mode has one half cycle of variation vertically within the substrate, while the TM_2 mode has one cycle of variation.) It can be seen that the full-wave results for both the normalized phase and attenuation constants are almost superimposed with the homogenized-model results. In particular, for propagation parallel to the wires, the agreement is independent of frequency in the range shown, whereas it tends to slightly deteriorate as the frequency increases for propagation orthogonal to the wires.

The frequencies for which $\beta = \alpha$ (i.e., 6.8 GHz for the TM_1 mode and 7.4 GHz for the TM_2 mode) correspond to frequencies of optimum broadside radiation from the leaky modes [19]. At these frequencies, the electrical thickness of the slab ($2h/\lambda_z$) is 0.45 and 0.90, respectively. The slab is essentially operating as a leaky parallel-plate waveguide, where the air region surrounding the slab presents a low impedance relative to the high-impedance slab material (which has a low permittivity).
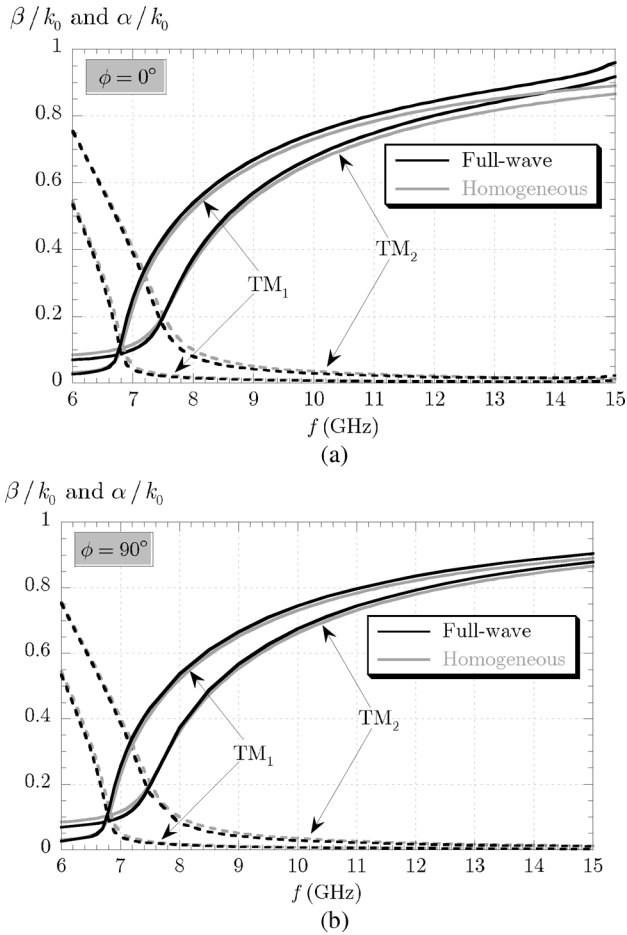
Fig. 3. Dispersion curves for the dominant even (TM_1) and odd (TM_2) leaky modes supported by a wire-medium slab in air, propagating in the directions: (a) $\phi = 0°$ and (b) $\phi = 90°$. *Solid lines*: phase constant. *Dashed lines*: attenuation constant. *Black lines*: full-wave MoM results. *Gray lines*: homogenized-model results. *Parameters*: $d_x = d_z = 10$ mm, $a = 0.1$ mm, $N = 8$ (homogenized parameters: $2h = 80$ mm, $k_p = 138.094$ rad/m).
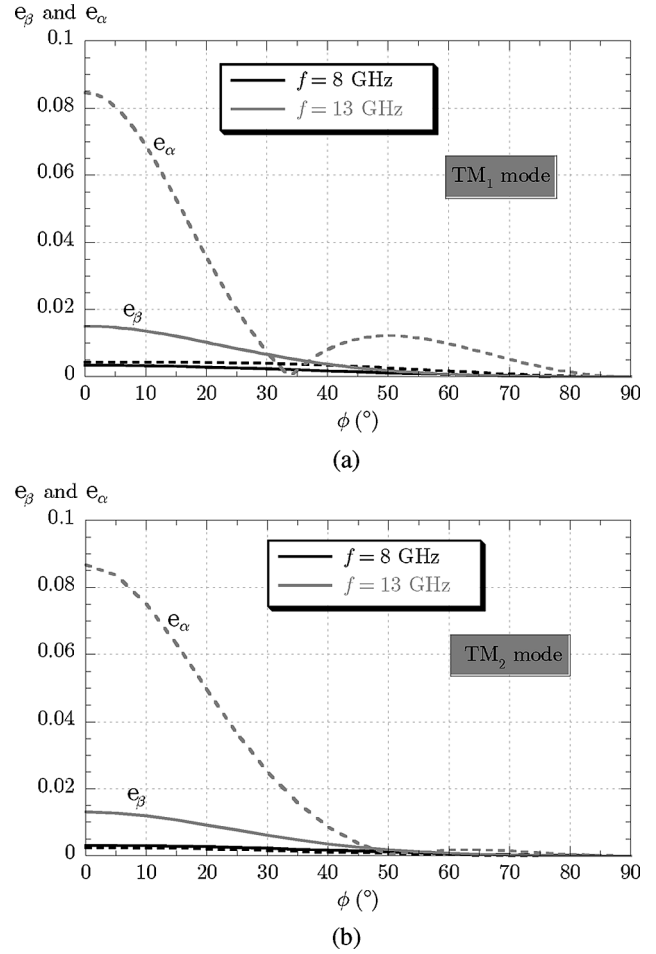

Fig. 4. Illustration of the degree of omnidirectionality of modal propagation. The relative errors e_β and e_α (defined as the normalized difference between the values of the phase and attenuation constants at an arbitrary propagation angle ϕ and those at $\phi = 90°$) are reported as a function of ϕ at two different frequencies for a structure, as in Fig. 3. (a) Fundamental TM_1 even mode. (b) Fundamental TM_2 odd mode. *Black lines*: 8 GHz. *Gray lines*: 13 GHz. *Solid lines*: e_β. *Dashed lines*: e_α.

For an ideal parallel-plate waveguide (with top and bottom metal walls), the electrical thickness of the waveguide would be exactly 0.5 and 1.0 for the TM_1 and TM_2 modes at cutoff, with cutoff corresponding to radiation at broadside (when radiation is allowed to escape from the waveguide so that the waveguide becomes leaky).

The degree of omnidirectionality of modal propagation achieved in actual periodic wire-medium slabs can be appreciated in Fig. 4. Here, the relative errors e_β and e_α for the phase and attenuation constants, defined as $e_\beta(\phi) = |\beta(\phi) - \beta(90°)|/\beta(90°)$ and $e_\alpha(\phi) = |\alpha(\phi) - \alpha(90°)|/\alpha(90°)$, are reported as a function of the propagation angle ϕ for both the fundamental even and odd modes of a structure, as in Fig. 3. It can be seen that for low frequencies (e.g., at $f = 8$ GHz), the maximum relative error in the entire angular range is less than 1%, indicating a very high degree of omnidirectionality of modal propagation. In the high-frequency range (e.g., at $f = 13$ GHz), the maximum relative error for the attenuation constant e_β is still also less than 2%, while the attenuation constant starts to lose its isotropic character (although its maximum relative error e_α is less than 10%).

The effect of changing the spatial periods of the wire lattice has also been investigated, maintaining the condition of thin wires [i.e., $a \ll \min(d_x, d_z)$]. In Fig. 5, a comparison between full-wave and homogenized results is presented for the fundamental TM_2 odd mode of a structure, as in Fig. 3, with the spatial period $d_x = d_z = d$ reduced from 10 to 3 mm, propagating in the principal directions $\phi = 0°$ and $\phi = 90°$. As expected, the dispersion curves are shifted towards a higher frequency range with respect to those in Fig. 3; in fact, one effect of reducing the spatial period in a square lattice is to increase the plasma wavenumber. Moreover, although the spatial period is smaller with respect to that of the structure considered in Fig. 3, the period-wavelength ratio has increased so that the accuracy of the homogenized model is decreased; however, overall it remains very good. The small difference between the solid black curves ($\phi = 0$ and $\phi = 90°$) shows that the degree of omnidirectionality also tends to reduce at high frequencies (above approximately 40 GHz).

It is also interesting to consider the effect of letting the spatial periods along the x- and z-directions be different, i.e., $d_x \neq d_z$, maintaining fixed the other parameters (i.e., the wire radius a
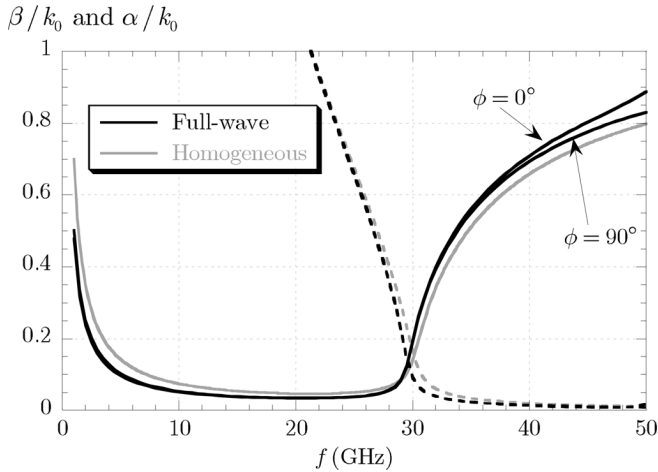
Fig. 5. Effect of reducing the period of the wire medium. Dispersion curve of the fundamental TM_2 odd leaky mode of a structure, as in Fig. 3, with $d_x = d_z = d = 3$ mm. *Solid lines*: phase constant. *Dashed lines*: attenuation constant.
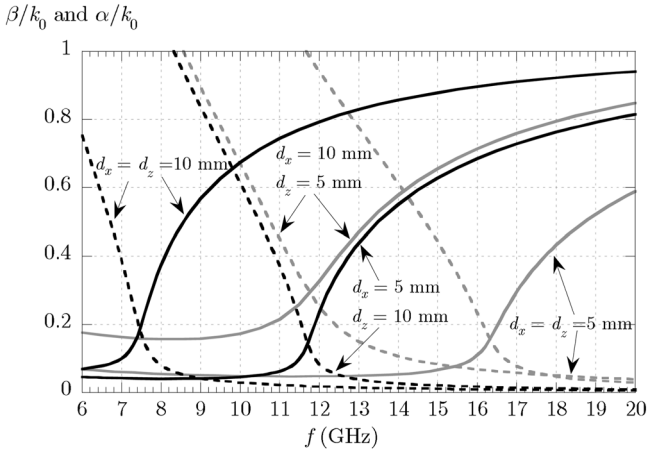

Fig. 6. Effect of different wire spacings along x and z in the wire-medium slab. Dispersion curves of the fundamental TM_2 odd mode supported by a structure, as in Fig. 3, are shown for different values of the spatial periods d_x and d_z. *Solid lines*: phase constant. *Dashed lines*: attenuation constant.

and the number of wire layers N). In Fig. 6, dispersion curves are shown for the fundamental TM_2 odd mode propagating at $\phi = 90°$ on four different wire-medium slabs, two with a square lattice ($d_x = d_z = 10$ mm and $d_x = d_z = 5$ mm) and two with a rectangular lattice ($d_x = 10$ mm, $d_z = 5$ mm and $d_x = 5$ mm and $d_z = 10$ mm). In all cases, the simulations are in very good agreement with the homogenized results (not reported for clarity). In particular, the frequencies at which $\beta = \alpha$ are always well predicted by the simple formula $f_{\beta=\alpha} = \sqrt{f_p^2 + c^2/(2h)^2}$ [19], where h is the equivalent thickness of the homogenized model, c is the speed of light, and $f_p = k_p c/(2\pi)$ is the plasma frequency calculated according to (2) and (3). The values for β/k_0 and α/k_0 at $f = f_{\beta=\alpha}$ given by the approximate formula $\sqrt{c^3/(8\pi f_p^3 h^3)}$ [19] are also very accurate. It can be seen that by decreasing the wire spacing d_z, the equivalent thickness h decreases, thus increasing the value of β (and α) at $f = f_{\beta=\alpha}$; on the other hand, decreasing the wire spacing d_x decreases the value of β (and α) at $f = f_{\beta=\alpha}$. Since these value determine
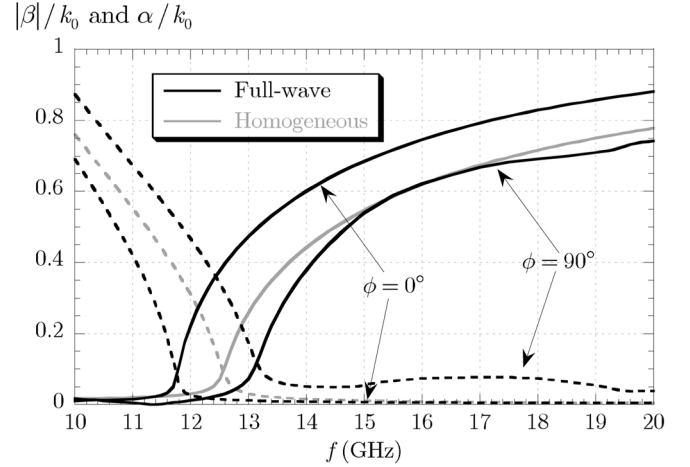

Fig. 7. Effect of dropping the assumption of thin wires. Dispersion curves of the fundamental odd leaky mode supported by a structure, as in Fig. 3, with wire radius $a = 1$ mm, propagating at $\phi = 0°$ and $\phi = 90°$. *Black lines*: full-wave MoM results. *Gray lines*: homogenized model. *Solid lines*: phase constant. *Dashed lines*: attenuation constant.

the directivity of the beam radiated at broadside by the structure excited by a simple source (e.g., a dipole), these parameters can provide a further degree of freedom in order to obtain a desired directivity at a given frequency when the wire-medium slab is used in antenna applications.

Finally, when the assumption of thin wires is dropped, the homogenization procedure cannot be based on (1) for the dyadic permittivity. In this case, the modal propagation is not omnidirectional anymore, as can be observed in Fig. 7, where dispersion curves are reported for the fundamental odd mode supported by a structure, as in Fig. 3, but with a wire radius ten times larger, i.e., $a = 1$ mm. A large discrepancy can be observed between the dispersion curves in the two propagation directions $\phi = 0°$ and $\phi = 90°$ (*black lines*); furthermore, the homogenized results based on (1) (*gray lines*) are azimuthally omnidirectional and do not provide accurate results, as expected.

It may be interesting to note that, at $f \simeq 11.4$ GHz, the phase constant becomes equal to zero for propagation at $\phi = 90°$ so that, at frequencies lower than 11.4 GHz, the phase constant would be negative (it is reported in absolute value in Fig. 7). This means that the pole of the spectral Green's function of the structure corresponding to the considered leaky mode has crossed the negative vertical axis of the complex k_ρ plane; hence, it has crossed a Sommerfeld branch cut and has moved to a proper sheet of the involved Riemann surface; physically, this corresponds to a transition from a forward to a backward regime for the leaky mode.

B. Electric Field at the Air–Slab Interface

In this section, the electric field excited by a horizontal electric dipole placed inside a grounded wire-medium slab of thickness h is studied, adopting both the approximate homogenized model and a rigorous full-wave simulation of an actual truncated wire-medium structure. The horizontal electric dipole is assumed to be parallel to the wire direction and placed at a distance $h_s = h/2$ from the ground plane, equidistant from the four nearby metal wires. The tangential field is calculated on
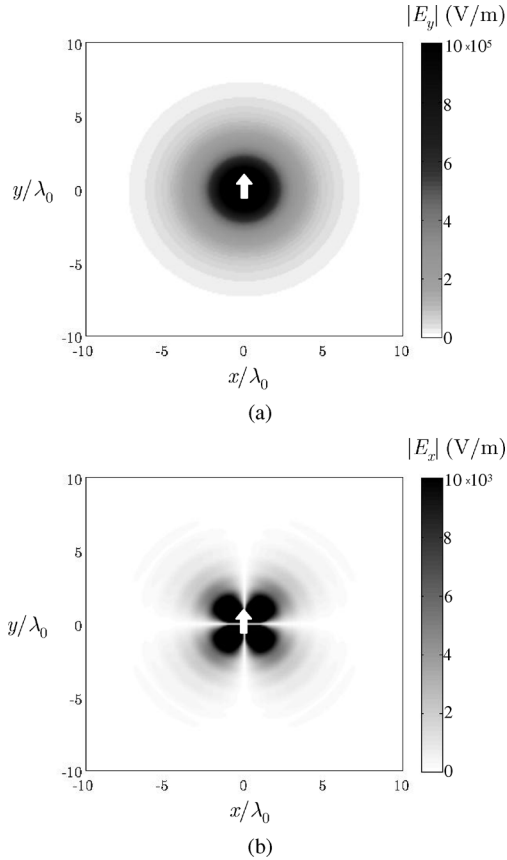
Fig. 8. Amplitude of the Cartesian components of the electric field at the air–slab interface of a grounded wire-medium slab excited by a horizontal electric dipole parallel to the wires, calculated with the homogenized model at $f = 4.07$ GHz. (a) E_y component. (b) E_x component. *Parameters* of the wire-medium structure: $d_x = d_z = 20$ mm, $a = 0.5$ mm, $N = 6$.

the plane $z = h$, i.e., at the air–slab interface in the homogenized model and at a distance $d_z/2$ from the center of the wires in the upper row in the actual wire-medium structure.

In Fig. 8, results obtained with the homogenized model are shown for an infinite grounded wire-medium slab with $d_x = d_z = 20$ mm, $a = 0.5$ mm, and $N = 6$ layers of wires (corresponding to homogenized parameters $h = Nd_z = 120$ mm and $f_p \simeq 3.88$ GHz) at the frequency $f = 4$ GHz. At this frequency, the dominant leaky mode is the TM_2 mode with nearly equal values for the normalized phase and attenuation constants $\beta/k_0 \simeq \alpha/k_0 \simeq 0.1$ such that it radiates a narrow pencil beam with maximum power density at broadside [11]. As explained in Section II-C, the total field at the air–slab interface has been calculated through a numerical evaluation of the integrals in (12) and (13). In Fig. 8(a), the amplitude of the E_y component (*parallel* to the wires) is shown. As expected from the discussion in Section II-C, the amplitude of this component is almost perfectly independent of the azimuthal angle ϕ. On the other hand, the amplitude of the E_x component (*orthogonal* to the wires) is seen in Fig. 8(b) to be approximately two orders of magnitude lower than the amplitude of E_y, thus confirming that the field at the air–slab interface is essentially linearly polarized along the wire direction.

As discussed in Section II-C, the total field on the aperture consists of the leaky-mode field and the space-wave field. For a
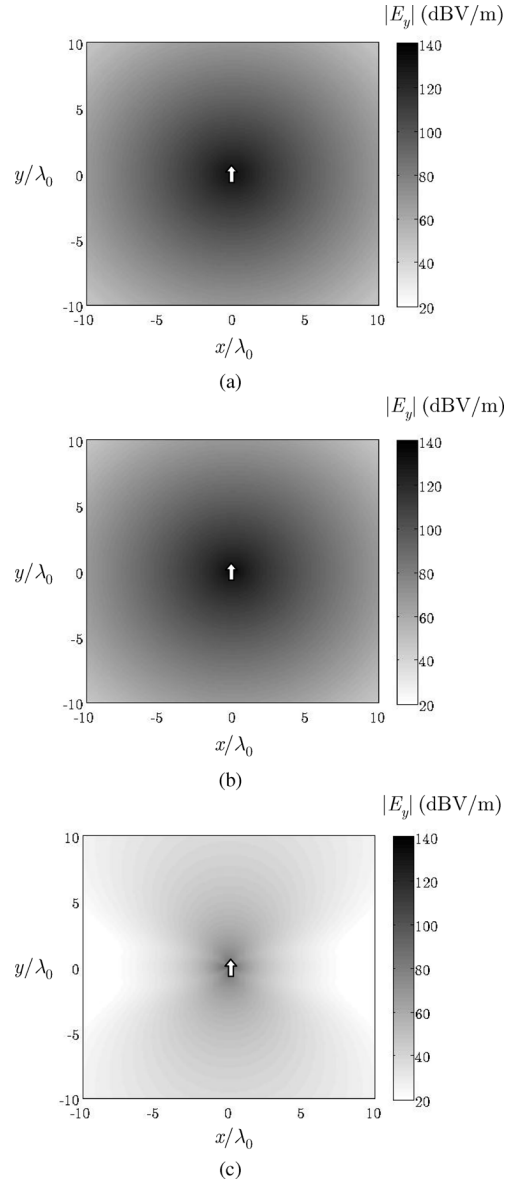

Fig. 9. Amplitude (in dBV/m) of the y component of the electric field at the air–slab interface for the same structure considered in Fig. 8 at $f = 4.07$ GHz. (a) Total field. (b) Leaky-wave field. (c) Space-wave field.

low-permittivity slab that is optimized for maximum radiation at broadside (as in Fig. 8), the leaky-mode field is expected to dominate the total field of the aperture. To verify this, results are shown in Figs. 9 and 10 for the leaky-mode field and the space-wave field on the aperture for the case shown in Fig. 8 for the co-polarized (y) and cross-polarized fields (x), respectively. The leaky-mode field and space-wave field have been numerically evaluated, as explained in Section II-C. The total field on the aperture is also shown, plotted on the same scale as the leaky-mode and space-wave fields for an easy comparison.

Fig. 9 verifies that the leaky-mode field is the dominant contributor to the co-polarized field of the aperture with the amplitude of the co-polarized space-wave field being on the order of 50 dB lower. On the other hand, Fig. 10 shows that the space-wave contribution to the cross-polarized field on the aperture is not negligible, its amplitude being comparable (but a bit weaker)
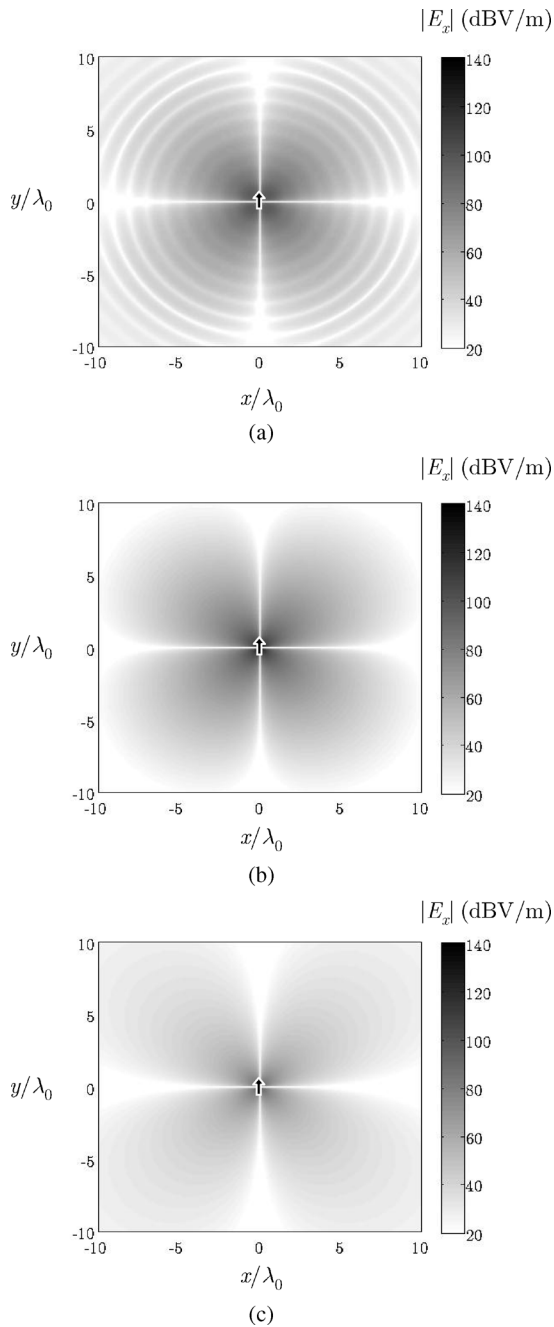
Fig. 10.   Amplitude (in dBV/m) of the x component of the electric field at the air–slab interface for the same structure considered in Fig. 8 at $f = 4.07$ GHz. (a) Total field. (b) Leaky-wave field. (c) Space-wave field.

Fig. 11.   Amplitude (in dBV/m) of the co-polarized (E_y) and cross-polarized (E_x) electric fields of the leaky mode at the air–slab interface as a function of the normalized distance ρ/λ_0 from the source along the $\phi = 45°$ line for the same structure considered in Fig. 8 at $f = 4.07$ GHz.

Fig. 12.   Amplitude (in dBV/m) of the co-polarized (E_y) and cross-polarized (E_x) electric fields of the space wave at the air–slab interface as a function of the normalized distance ρ/λ_0 from the source along the $\phi = 45°$ line for the same structure considered in Fig. 8 at $f = 4.07$ GHz.

with that of the leaky-mode contribution (with the cross-polarized field of both the leaky mode and the space-wave field vanishing along the principal axes); this gives rise to some oscillations in the cross-polarized component of the total field.

The co-polarized field of the leaky mode is almost perfectly omnidirectional in azimuth, as expected. The co-polarized field of the space-wave field is instead maximum in the wire direction (i.e., along the y-axis), while it decays more rapidly orthogonally to the wires (i.e., along the x-direction). The cross-polarized fields of both the leaky-mode field and the space-wave field are maximum in the diagonal planes, and zero along the principal axes.
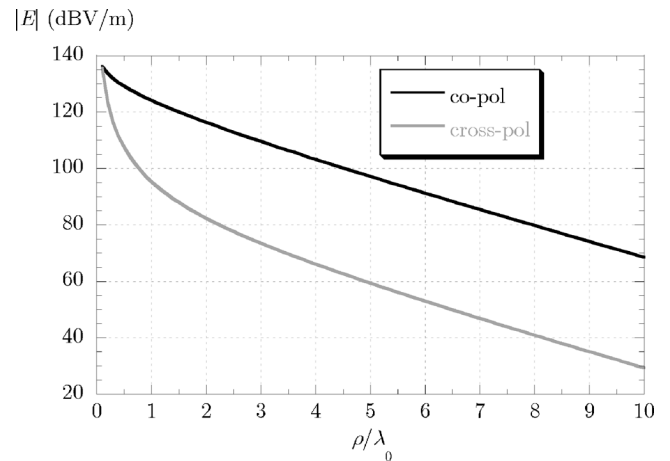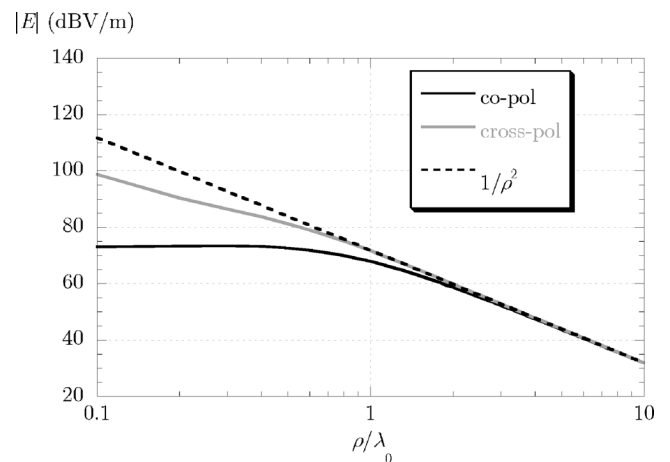
Fig. 11 shows a plot of the co-polarized and cross-polarized aperture fields of the leaky mode versus distance from the source at a fixed angle of $\phi = 45°$. On this scale, it is obvious that both the co-polarized and cross-polarized leaky-mode fields decay exponentially, as expected.

Fig. 12 investigates the behavior of the space-wave field on the aperture, showing both the co-polarized and the cross-polarized fields together with a reference curve that is a plot of a normalized $1/\rho^2$ function along the $\phi = 45°$ line. It is seen that the space-wave field is mainly cross-polarized near the source, but further away the co-polarized and cross-polarized fields have almost the same amplitude, and both decay as $1/\rho^2$. This decay rate is the same as is observed for sources in the presence of general layered media, such as a dipole over a dielectric half-space.

Due to the different decay rates, the amplitude of the space-wave field will eventually surpass that of the leaky-mode field far away from the source, but this occurs at a distance of approximately 18.5 wavelengths, and is off the scale shown in the figures. This explains why the broadside radiation from such a structure is mainly due to the leaky mode [9]–[11]. The leaky
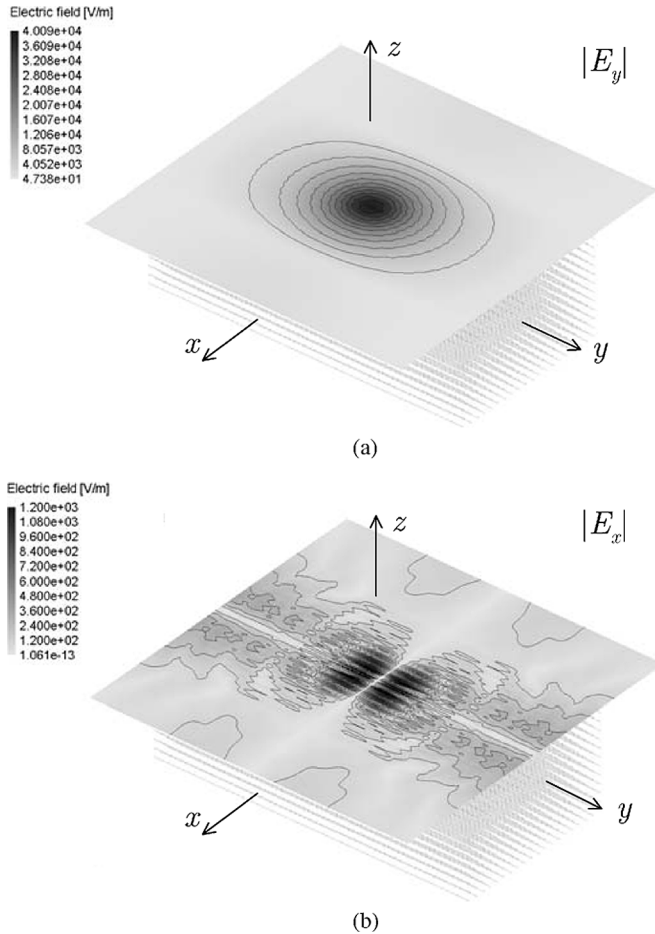
Fig. 13. Amplitude of the Cartesian components of the electric field at the air–slab interface of a truncated grounded wire-medium slab excited by a horizontal electric dipole, calculated with FEKO at $f = 4.07$ GHz. *Parameters*: as in Fig. 8.

mode is very dominant because the dipole source is located inside the homogenized wire-medium (low-permittivity) slab at the optimum location (in the middle of the slab) to best excite the leaky mode, while also minimizing the space-wave field. Other results (not shown) reveal that, when the dipole is located near the interface, the leaky mode becomes somewhat weaker and the space-wave field becomes much stronger so that the two now have comparable amplitudes over the range of distances shown in Figs. 11 and 12.

As mentioned in Section II-C, the use of a homogenized model for calculating the near field excited by a finite source may be questionable since this model cannot take into account the microscopic near-field interaction of the source with the lattice (hence, it would not provide reliable results for the input impedance of a more realistic source). To assess the validity of the above conclusions about the features of the field at the air–slab interface, an actual wire-medium structure has then been simulated with a general-purpose commercial software tool (FEKO) based on the MoM in the spatial domain. A truncated slab with the same parameters as in Fig. 8 has been considered with a finite extension in the xy-plane equal to $5\lambda_0 \times 5\lambda_0$. In Fig. 13(a), the amplitude of the E_y component is reported with a grayscale map and equiamplitude contour

lines on the plane $z = h$; it can be observed that E_y is indeed substantially independent of the azimuthal angle until we get further away. In Fig. 13(b), the E_x component is reported; here the microscopic structure of the near field is clearly apparent, which is not visible in the corresponding homogenized results in Fig. 8(b). However, it is confirmed that the E_x component is dominated in magnitude by the E_y component, although the difference between the two is only one order of magnitude in the full-wave results.

In conclusion, when a single dominant leaky mode is excited, the aperture field at the air–slab interface is almost perfectly linearly polarized with an omnidirectional amplitude, and the homogenized slab model, although not able to capture the fine details of the near field, correctly predicts such qualitative features. It is worth noting that these features are typical of planar leaky-wave antennas based on conventional designs when optimized for broadside radiation (see, e.g., [20], where a substrate–superstrate configuration is analyzed); however, for conventional designs, these features are due to the excitation of *a pair* of TE_z and TM_z leaky modes, whereas a *single* TM_y leaky mode is excited in the present wire-medium configuration.

V. CONCLUSION

Modal propagation and excitation on a wire-medium slab in free space have been investigated through both a homogenized model of the wire medium, which takes into account both anisotropy and spatial dispersion, and rigorous full-wave simulations.

The homogenized analysis has lead to the result that modal propagation is omnidirectional, i.e., independent of the propagation angle along the slab, and that surface waves cannot exist. A parametric analysis of the dispersion features of the leaky modes has been presented to illustrate the degree of modal omnidirectionality as a function of the geometrical parameters of the wire medium and of frequency.

The excitation of a grounded wire-medium slab by means of a horizontal electric dipole has also been studied. The main features of the field at the air–slab interface, i.e., its character of being almost perfectly linearly polarized along the wire direction and omnidirectional in magnitude, have been ascertained through a MoM simulation of an actual truncated wire-medium structure, and have been shown to be correctly predicted by the approximate homogenized model.

Future investigations will concern the input-impedance properties of more realistic sources placed inside the considered wire-medium slabs, and they will necessarily require the rigorous treatment of the near-field interaction between the source and metal wires through full-wave simulations of the actual periodic material.

APPENDIX
EQUIVALENT TRANSMISSION LINES FOR TE_y AND TM_y FIELDS

Here, the transverse equivalent networks in the z-direction are derived for TE_y and TM_y waves inside an electrically uniaxial medium with a spatially and temporally dispersive permittivity, as in (1), starting from the spectral form of Maxwell's equations and taking into account the presence of impressed electric and magnetic currents.

By Fourier transforming the Maxwell equations with respect to x and y, we have

$$\begin{cases} -jk_y\tilde{E}_z - \dfrac{\partial \tilde{E}_y}{\partial z} = -j\omega\mu\tilde{H}_x - \tilde{M}_x \\ \dfrac{\partial \tilde{E}_x}{\partial z} + jk_x\tilde{E}_z = -j\omega\mu\tilde{H}_y - \tilde{M}_y \\ -jk_x\tilde{E}_y + jk_y\tilde{E}_x = -j\omega\mu\tilde{H}_z - \tilde{M}_z \end{cases} \quad (21)$$

$$\begin{cases} -jk_y\tilde{H}_z - \dfrac{\partial \tilde{H}_y}{\partial z} = j\omega\epsilon_0\varepsilon_{\rm rt}\tilde{E}_x + \tilde{J}_x \\ \dfrac{\partial \tilde{H}_x}{\partial z} + jk_x\tilde{H}_z = j\omega\epsilon_0\varepsilon_{ryy}\tilde{E}_y + \tilde{J}_y \\ -jk_x\tilde{H}_y + jk_y\tilde{H}_x = j\omega\epsilon_0\varepsilon_{\rm rt}\tilde{E}_z + \tilde{J}_z. \end{cases} \quad (22)$$

In the TE_y case, $\tilde{E}_y = 0$ and $\tilde{J}_y = 0$, and by simple manipulations of (21) and (22), it is possible to express all the remaining field components in terms of $\tilde{E}_x$ and $\tilde{H}_y$ and of the impressed currents. The second equation of (21) and the first equation of (22) can then be written as transmission line equations

$$\begin{cases} \dfrac{\mathrm{d}V^{\rm TE}}{\mathrm{d}z} = -Z_{\rm s}^{\rm TE}I^{\rm TE} + v^{\rm TE} \\ \dfrac{\mathrm{d}I^{\rm TE}}{\mathrm{d}z} = -Y_{\rm p}^{\rm TE}V^{\rm TE} + i^{\rm TE} \end{cases} \quad (23)$$

where

$$\begin{aligned} V^{\rm TE} &= \tilde{E}_x \\ I^{\rm TE} &= \tilde{H}_y \\ Z_{\rm s}^{\rm TE} &= j\omega\mu\left(1 - \frac{k_x^2}{k_0^2\varepsilon_{\rm rt} - k_y^2}\right) \\ Y_{\rm p}^{\rm TE} &= \frac{j}{\omega\mu}\left(k_0^2\varepsilon_{\rm rt} - k_y^2\right) \\ v^{\rm TE} &= \frac{\omega\mu k_x}{k_0^2\varepsilon_{\rm rt} - k_y^2}\tilde{J}_z - \frac{k_x k_y}{k_0^2\varepsilon_{\rm rt} - k_y^2}\tilde{M}_x + \tilde{M}_y \\ i^{\rm TE} &= -\frac{k_y}{\omega\mu}\tilde{M}_z - \tilde{J}_x. \end{aligned} \quad (24)$$

The propagation constant and characteristic impedance of the TE_x equivalent transmission line are then

$$\begin{aligned} k_z^2 &= -Z_{\rm s}^{\rm TE}Y_{\rm p}^{\rm TE} = k_0^2\varepsilon_{\rm rt} - k_x^2 - k_y^2 \\ Z_{\rm c}^{\rm TE} &= \sqrt{\frac{Z_{\rm s}^{\rm TE}}{Y_{\rm p}^{\rm TE}}} = k_0\eta_0\frac{k_z}{\varepsilon_{\rm rt}k_0^2 - k_y^2}. \end{aligned} \quad (25)$$

Note that, by letting $\beta_{\rm o} = \sqrt{k_x^2 + k_y^2 + k_z^2}$, from the first equation of (25), it is inferred that

$$\beta_{\rm o} = k_0\sqrt{\varepsilon_{\rm rt}}. \quad (26)$$

Hence, the normalized phase constant $\beta_{\rm o}/k_0$ (i.e., the effective index $n_{\rm o}$) of a uniform TE_y plane wave (i.e., an *ordinary* wave) inside the considered medium is equal to $\sqrt{\varepsilon_{\rm rt}}$ regardless of its direction of propagation, as expected.

In the TM_y case, $\tilde{H}_y = 0$ and $\tilde{M}_y = 0$; reasoning as in the TE_y case, the first equation of (21), and the second equation

of (22) can then be written as transmission line equations, as in (23), but with a TM superscript where

$$\begin{aligned} V^{\rm TM} &= \tilde{E}_y \\ I^{\rm TM} &= -\tilde{H}_x \\ Z_{\rm s}^{\rm TM} &= \frac{j}{\omega\epsilon_0\varepsilon_{\rm rt}}\left(k_0^2\varepsilon_{\rm rt} - k_y^2\right) \\ Y_{\rm p}^{\rm TM} &= j\omega\epsilon_0\left(\varepsilon_{ryy} - \frac{\varepsilon_{\rm rt}k_x^2}{k_0^2\varepsilon_{\rm rt} - k_y^2}\right) \\ v^{\rm TM} &= \frac{k_y}{\omega\epsilon_0\varepsilon_{\rm rt}}\tilde{J}_z + \tilde{M}_x \\ i^{\rm TM} &= \frac{k_x k_y}{k_0^2\varepsilon_{\rm rt} - k_y^2}\tilde{J}_x - \frac{\omega\epsilon_0\varepsilon_{\rm rt}k_x}{k_0^2\varepsilon_{\rm rt} - k_y^2}\tilde{M}_z - \tilde{J}_y. \end{aligned} \quad (27)$$

The propagation constant and characteristic impedance of the TM_y equivalent transmission line are then

$$\begin{aligned} k_z^2 &= -Z_{\rm s}^{\rm TM}Y_{\rm p}^{\rm TM} \\ &= k_0^2\left[\varepsilon_{ryy} + \left(1 - \frac{\varepsilon_{ryy}}{\varepsilon_{\rm rt}}\right)\left(\frac{k_y}{k_0}\right)^2\right] - k_x^2 - k_y^2 \\ Z_{\rm c}^{\rm TM} &= \frac{\eta_0}{k_0}\frac{\varepsilon_{\rm rt}k_0^2 - k_y^2}{\varepsilon_{\rm rt}k_z}. \end{aligned} \quad (28)$$

Again, by letting $\beta_{\rm e} = \sqrt{k_x^2 + k_y^2 + k_z^2}$, one obtains from the first equation of (28) and (1)

$$\beta_{\rm e} = k_0\sqrt{\varepsilon_{ryy} + \left(1 - \frac{\varepsilon_{ryy}}{\varepsilon_{\rm rt}}\right)\left(\frac{k_y}{k_0}\right)^2} = k_0\sqrt{\varepsilon_{\rm rh} - \frac{k_{\rm p}^2}{k_0^2}}. \quad (29)$$

From (29), it is concluded that the normalized phase constant $\beta_{\rm e}/k_0$ (i.e., the effective index $n_{\rm e}$) of a uniform TM_y plane wave (i.e., an *extraordinary* wave) inside the considered medium is equal to $\sqrt{\varepsilon_{\rm rh} - k_{\rm p}^2/k_0^2}$, regardless of its direction of propagation. The fact that $\beta_{\rm e}$ is independent of the direction of propagation is a consequence of the spatially dispersive model adopted for the effective medium and expressed by (1), as observed in [3].

REFERENCES

[1] J. Brown, "Artificial dielectrics having refractive indexes less than unity," *Proc. Inst. Elect. Eng.*, vol. 100, pp. 51–62, May 1953.

[2] G. Shvets, "Photonic approach to making a surface wave accelerator," in *Proc. 10th Adv. Accelerator Concepts Workshop*, 2002, vol. CP647, pp. 371–382.

[3] P. A. Belov, R. Marqués, S. I. Maslovski, I. S. Nefedov, M. Silveirinha, C. R. Simovski, and S. A. Tretyakov, "Strong spatial dispersion in wire media in the very large wavelength limit," *Phys. Rev. B, Condens. Matter*, vol. 67, pp. 113103-1–113103-4, 2003.

[4] C. R. Simovski and P. A. Belov, "Low-frequency spatial dispersion in wire media," *Phys. Rev. E, Stat. Phys. Plasmas Fluids Relat. Interdiscip. Top.*, vol. 70, pp. 046616-1–046616-8, Oct. 2004.

[5] M. G. Silveirinha and C. A. Fernandes, "Homogenization of 3-D-connected and nonconnected wire metamaterial," *IEEE Trans. Microw. Theory Tech.*, vol. 53, no. 4, pp. 1418–1430, Apr. 2005.

[6] M. G. Silveirinha, "Additional boundary condition for the wire medium," *IEEE Trans. Antennas Propag.*, vol. 54, no. 6, pp. 1766–1780, Jun. 2006.

[7] I. S. Nefedov, A. J. Viitanen, and S. A. Tretyakov, "Propagating and evanescent modes in two-dimensional wire media," *Phys. Rev. E, Stat. Phys. Plasmas Fluids Relat. Interdiscip. Top.*, vol. 71, pp. 046612-1–046612-10, 2005.

[8] I. S. Nefedov and A. J. Viitanen, "Guided waves in uniaxial wire medium slab," *PIER*, vol. 51, pp. 167–185, 2003.

[9] P. Burghignoli, G. Lovat, F. Capolino, D. R. Jackson, and D. R. Wilton, "3D directive radiation from a horizontal dipole embedded in a homogenized grounded wire-medium slab," in *IEEE AP-S Conf. Dig.*, Albuquerque, NM, Jul. 9–14, 2006, pp. 2989–2992.

[10] P. Burghignoli, G. Lovat, F. Capolino, D. R. Jackson, and D. R. Wilton, "Leaky modes on a grounded wire-medium slab," in *IEEE MTT-S Int. Microw. Symp. Dig.*, Honolulu, HI, Jun. 3–8, 2007, pp. 1663–1666.

[11] P. Burghignoli, G. Lovat, F. Capolino, D. R. Jackson, and D. R. Wilton, "Directive leaky-wave radiation from a dipole source in a wire-medium slab," *IEEE Trans. Antennas Propag.*, vol. 56, no. 5, May 2008, to be published.

[12] P. A. Belov, S. A. Tretyakov, and A. J. Viitanen, "Dispersion and reflection properties of artificial media formed by regular lattices of ideally conducting wires," *J. Electromagn. Waves Applicat.*, vol. 16, pp. 1153–1170, Sep. 2002.

[13] G. Guida, D. Maystre, G. Tayeb, and P. Vincent, "Mean-field theory of two-dimensional metallic photonic crystals," *J. Opt. Soc. Amer. B, Opt. Phys.*, vol. 15, pp. 2308–2315, 1998.

[14] P. Baccarelli, P. Burghignoli, F. Frezza, A. Galli, P. Lampariello, G. Lovat, and S. Paulotto, "Fundamental modal properties of surface waves on metamaterial grounded slabs," *IEEE Trans. Microw. Theory Tech.*, vol. 53, no. 4, pp. 1431–1442, Apr. 2005.

[15] F. Capolino, D. R. Jackson, D. R. Wilton, and L. B. Felsen, "Comparison of methods for calculating the field excited by a dipole near a 2-D periodic material," *IEEE Trans. Antennas Propag.*, vol. 55, no. 6, pp. 1644–1655, Jun. 2007.

[16] F. Capolino, D. R. Wilton, and W. A. Johnson, "Efficient calculation of the 2-D Green's function for 1-D periodic structures using the Ewald method," *IEEE Trans. Antennas Propag.*, vol. 53, no. 9, pp. 2977–2984, Sep. 2005.

[17] W. Chew, *Waves and Fields in Inhomogeneous Media*. Piscataway, NJ: IEEE Press, 1995.

[18] A. Hessel, "Travelling-wave antennas," in *Antenna Theory*, R. E. Collin and F. J. Zucker, Eds. New York: McGraw-Hill, 1969, ch. 19, pt. 2.

[19] G. Lovat, P. Burghignoli, F. Capolino, D. R. Jackson, and D. R. Wilton, "Analysis of directive radiation from a line source in a metamaterial slab with low permittivity," *IEEE Trans. Antennas Propag.*, vol. 54, no. 3, pp. 1017–1030, Mar. 2006.

[20] A. Polemi and S. Maci, "On the polarization properties of a dielectric leaky wave antenna," *IEEE Antennas Wireless Propag. Lett.*, vol. 5, no. 1, pp. 306–310, Dec. 2006.

Giampiero Lovat (S'02–M'06) was born in Rome, Italy, on May 31, 1975. He received the Laurea degree (*cum laude*) in electronic engineering and Ph.D. degree in applied electromagnetics from "La Sapienza" University of Rome, Rome, Italy, in 2001 and 2004, respectively.

In 2005, he joined the Electrical Engineering Department, "La Sapienza" University of Rome, where he is currently an Associate Researcher. From January 2004 to July 2004, he was a Visiting Scholar with the University of Houston, Houston, TX. He coauthored a book on electromagnetic shielding. His current research interests include leaky-wave antennas, periodic structures, complex media, and electromagnetic shielding.

Dr. Lovat was the recipient of the 2005 Young Scientist Award presented at the URSI General Assembly, New Delhi, India.

Filippo Capolino (S'94–M'97–SM'04) was born in Florence, Italy, in 1967. He received the Laurea degree (*cum laude*) in electronic engineering and Ph.D. degree from the University of Florence, Florence, Italy, in 1993 and 1997, respectively.

He is currently an Assistant Professor with the Department of Information Engineering, University of Siena, Siena, Italy. From 1997 to 1998, he was a Fulbright Research Visitor with the Department of Aerospace and Mechanical Engineering, Boston University, Boston, MA, where he continued his research under a grant from the Italian National Council for Research (CNR) from 1998 to 1999. From 2000 to 2001, he was a Research Assistant Visiting Professor with the Department of Electrical and Computer Engineering, University of Houston, Houston, TX, where he is currently an Adjunct Assistant Professor. From November to December 2003, he was an Invited Assistant Professor with the Institut Fresnel, Marseille, France. He is an Associate Editor for the new Elsevier journal *Metamaterials*. His research interests include theoretical and applied electromagnetics focused on high-frequency short-pulse radiation, array antennas, periodic structures, numerical modeling, and metamaterials.

Dr. Capolino is the Coordinator of the Metamorphose EU Doctoral Programmes on Metamaterials. He is an associate editor for the IEEE TRANSACTIONS ON ANTENNAS AND PROPAGATION. He was the recipient of the 1994 MMET'94 Student Paper Competition Award, the 1996 and 2006 Raj Mittra Travel Grant for Young Scientists, the 1996 "Barzilai" Prize for the best paper presented at the National Italian Congress of Electromagnetism (XI RiNEm), and a 1998 Young Scientist Award for participating in the URSI International Symposium on Electromagnetic Theory. He was also the recipient of the R. W. P. King Prize Paper Award presented by the IEEE Antennas and Propagation Society for the Best Paper of 2000 by an author under the age of 36.

Paolo Burghignoli (S'97–M'01–SM'08) was born in Rome, Italy, on February 18, 1973. He received the Laurea degree (*cum laude*) in electronic engineering and Ph.D. degree in applied electromagnetics from "La Sapienza" University of Rome, Rome, Italy, in 1997 and 2001, respectively.

In 1997, he joined the Electronic Engineering Department, "La Sapienza" University of Rome, where he is currently an Associate Researcher. From January 2004 to July 2004, he was a Visiting Research Assistant Professor with the University of Houston, Houston, TX. His scientific interests include analysis and design of planar leaky-wave antennas, numerical methods for the analysis of passive guiding and radiating microwave structures, periodic structures, and propagation and radiation in metamaterials.

Dr. Burghignoli was the recipient of a 2003 IEEE Microwave Theory and Techniques Society (IEEE MTT-S) Graduate Fellowship, the 2005 Raj Mittra Travel Grant for Junior Researchers presented at the IEEE Antennas and Propagation Society Symposium, Washington, DC, and the 2007 "Giorgio Barzilai" Laurea Prize presented by the former IEEE Central & South Italy Section.

David R. Jackson (S'83–M'84–SM'95–F'99) was born in St. Louis, MO, on March 28, 1957. He received the B.S.E.E. and M.S.E.E. degrees from the University of Missouri, Columbia, in 1979 and 1981, respectively, and the Ph.D. degree in electrical engineering from the University of California at Los Angeles (UCLA), in 1985.

From 1985 to 1991, he was an Assistant Professor with the Department of Electrical and Computer Engineering, University of Houston, Houston, TX. From 1991 to 1998 he was an Associate Professor, and since 1998, he has been a Professor with this same department. He has also served as an Associate Editor for the *Journal of Radio Science* and the *International Journal of RF and Microwave Computer-Aided Engineering*. His current research interests include microstrip antennas and circuits, leaky-wave antennas, leakage and radiation effects in microwave integrated circuits, periodic structures, and electromagnetic compatibility (EMC).

Dr. Jackson is currently the chair of the Transnational Committee of the IEEE Antennas and Propagation Society (IEEE AP-S), and chair for URSI, U.S. Commission B. He is also on the Editorial Board of the IEEE TRANSACTIONS ON MICROWAVE THEORY AND TECHNIQUES. He was Chapter activities coordinator for the IEEE AP-S, a Distinguished Lecturer for the IEEE AP-S, an associate editor for the IEEE TRANSACTIONS ON ANTENNAS AND PROPAGATION, and a member of the IEEE AP-S Administrative Committee (AdCom).

Donald R. Wilton (S'63–M'65–SM'80–F'87–LF'08) was born in Lawton, OK, on October 25, 1942. He received the B.S., M.S., and Ph.D. degrees from the University of Illinois at Urbana-Champaign, in 1964, 1966, and 1970, respectively.

From 1965 to 1968, he was with the Hughes Aircraft Company, Fullerton, CA, where he was engaged in the analysis and design of phased-array antennas. From 1970 to 1983, he was with the Department of Electrical Engineering, University of Mississippi. Since 1983, he has been Professor of electrical engineering with the University of Houston, Houston, TX. From 1978 to 1979, he was a Visiting Professor with Syracuse University. From 2004 to 2005, he was a Visiting Scholar with the Polytechnic of Turin, Sandia National Laboratories, and the University of Washington. He has authored or coauthored many publications, lectured, and consulted extensively. His primary research interest is in computational electromagnetics.

Dr. Wilton has served as an associate editor for the IEEE TRANSACTIONS ON ANTENNAS AND PROPAGATION. He has also served the IEEE Antennas and Propagation Society (IEEE AP-S) as a Distinguished National Lecturer and as a member of their Administrative Committee (AdCom). He is also a member of Commission B, URSI, in which he has held various offices including chair of U.S. Commission B. He was the recipient of the IEEE Third Millennium Medal.